Preparation and Characterization of Rubber Blends for Industrial Tire Tread Fabrication

Article *in* International Journal of Polymer Science · August 2018

DOI: 10.1155/2018/2473286

Bismark Mensah
University of Ghana(Legon)
17 PUBLICATIONS **73** CITATIONS
SEE PROFILE

Benjamin Agyei-Tuffour
Rutgers, The State University of New Jersey
36 PUBLICATIONS **83** CITATIONS
SEE PROFILE

E. Nyankson
University of Ghana
27 PUBLICATIONS **193** CITATIONS
SEE PROFILE

Yaw Delali Bensah
University of Ghana
11 PUBLICATIONS **31** CITATIONS
SEE PROFILE

Hindawi
International Journal of Polymer Science
Volume 2018, Article ID 2473286, 12 pages
https://doi.org/10.1155/2018/2473286

Research Article

Preparation and Characterization of Rubber Blends for Industrial Tire Tread Fabrication

B. Mensah,[1,2] B. Agyei-Tuffour,[2] E. Nyankson,[2] Y. D. Bensah,[2] D. Dodoo-Arhin,[2] J. K. Bediako,[3] B. Onwona-Agyeman,[2] and A. Yaya[2]

[1] *932, Yun-Tech, ITECO 762, Deokpung-dong, Hanam-si, Gyeonggi-do, Republic of Korea*
[2] *Department of Materials Science and Engineering, CBAS, University of Ghana, Legon, Ghana*
[3] *Division of Semiconductor and Chemical Engineering, Chonbuk National University, Jeonju, Jeonbuk 561-756, Republic of Korea*

Correspondence should be addressed to A. Yaya; ayaya@ug.edu.gh

Received 7 June 2018; Revised 2 August 2018; Accepted 7 August 2018; Published 2 September 2018

Academic Editor: Domenico Acierno

The physico-mechanical properties of variable rubber blends including epoxide natural rubber (ENR), polybutadiene rubber (BR), and solution polymerized styrene-butadiene rubber (SBR) filled with silanized silica and carbon black mixtures were explored. The tensile, hardness, resilience, abrasion, and fatigue behavior were investigated. An optimized composition involving 30 phr of ENR and 70 phr SBR filled with mixtures of carbon blacks and silanized silica was proposed to be a suitable composition for the future development of green passenger truck tires, with low rolling resistance (fuel saving ability), high wear resistance, and desired fatigue failure properties.

1. Introduction

Environmental threats caused by excessive fuel consumption have been a major problem in the automobile industry. It is well established that an automobile consumes almost 30% of the energy for a drive on a highway [1, 2]. Thus, the automobile industry is obliged to reduce its portion accordingly through multifaceted approaches including the fabrication of new tires with less rolling resistances. Aerodynamics, nature of roads, the type of vehicle, and their engine capacity as well as other factors may contribute to fuel loses in a typical vehicle; however, rolling resistance (RR), which is associated with the material design, is the main cause of fuel loss in motor vehicles (a condition related to high CO_2 emission) [2, 3]. The RR is a property that is due to the visco-elastic behavior of the elastomer(s) used in making the tire/tread [3]. As illustrated in Figure 1, the rotation of the tire in the direction d, under the weight of the vehicle W, creates repeated cycles of deformation (region sitting on the road, i.e., y) and recovery (i.e., region x and z region) resulting in energy dissipation called hysteresis loss. This loss can be overcome by external works which give rise to RR [3, 4]. Also, the interaction of the tire with the road is a major contributing factor for road accidents. Thus, the interaction should provide adequate force (traction) for acceleration and braking to prevent slipping [3, 4]. Hence, a green tire/tread with fuel-saving capacity (lower RR, excellent traction (T), and abrasion resistance (AR)) is of great priority in tire engineering [4–7].

The type of matrix and filler used, filler dispersions, and their interactions (Filler-polymer and filler-filler interactions) are the main controlling factors to attain a composition intended for green tire manufacturing [3, 8, 9]. Over the past decades, high strength and resilient natural rubber (NR) filled with reinforcement such as carbon blacks (CB) and/or silica vulcanizates was widely explored for vehicle tire fabrication, but the one-matrix (NR-CB or NR-silica) composites have shown unsatisfactory results, as they failed to meet the green tire requirements owing to the fact that NR itself is susceptible to ozone fracturing with undesirable wear resistance (WR), RR, and TR properties [8, 10, 11]. Recently, engineered functional elastomers and active reinforcements

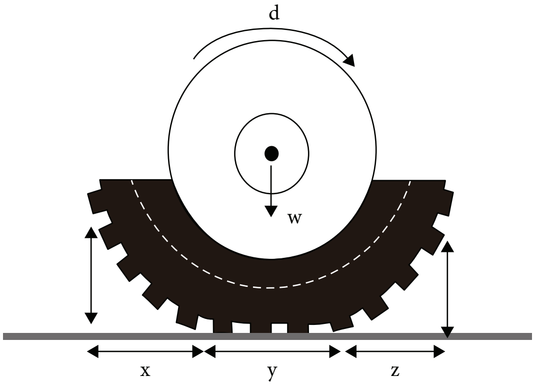

FIGURE 1: Illustration of the mechanism leading to hysteresis loss.

have been extensively investigated by various researchers aimed to attain efficient composition for the development of green tire/tread [7, 8, 10, 11]. In these attempts, blends of NR with at least one or more synthetic elastomers selected from the category of cis 1,4-polybutadiene (BR), NR/cis 1,4-polyisoprene rubber (IR), styrene-butadiene-based rubber (SBR), or their derivatives have been reinforced with mono or hybrid fillers such as CB and/or silanized silica as already demonstrated in previous studies [5, 7, 9]. The emergence of epoxidized natural rubber (ENR), which is reported to exhibit a higher polarity than NR, owing to the epoxide groups in its structure, has opened a new research area that seeks to examine its compatibility with silica for advanced applications including green tire fabrication [12, 13]. Sengloyluan et al. [14] have recently observed that increasing the mol% content of epoxide groups of ENR increases the tensile properties of ENR-silica-filled compounds than their counterpart NR silica-based compounds, although the curing times were prolonged. Other research [15] have also confirmed that ENR (epoxide group: 25% mol) had shown a glass transition temperature most suitable for tread application. They observed that ENR-silica tread compounds showed lower RR, hence reduced fuel consumption, with enhanced wet and ice traction compared with benchmark premium passenger or truck treads. Furthermore, Sarkawi et al. [12] had examined ENR-silica for the application of tire tread compound, in which ENR-silica was found to exhibit lower RR and better wet traction compared to NR-carbon black vulcanizates. However, there is currently little research work on ENR used as a component for green tire manufacturing. Nevertheless, a tire/tread generally constitutes a structure of various components with diverse properties and chemistry; hence, choosing each of these substances in their various amounts, the processing conditions and characterizations techniques adopted to arrive at conditions that satisfies the magic triangle of a green tire/tread (excellent WR and TR and low RR), has been a very challenging task. For this reason, further exploration in an attempt to obtain a composition for green tire/tread is inevitable. Presently, a detailed study on the blends of ENR, BR, and SSBR, with mixtures of carbon blacks and silanized silica, was investigated. The effect of maleic-anhydride (compatibilizer) on these blends was also examined. Wear resistance, flex fatigue life, hysteresis, tensile properties, and crosslinking densities were conducted to better understand the physico-mechanical properties of the vulcanizates. The current results present an optimized composition for green tire/tread preparation.

2. Experimental

2.1. Chemicals and Compound Formulation. In this study, ENR (epoxide group: 25–40% mol) was supplied by Doo Man Co. Ltd., South Korea; SSBR (SSBR-3323) was obtained from LG Chem, South Korea; and BR (BR-1208), carbon black N550 (with the specific surface of 95–105 m^2/g), and CORAX N330 (iodine adsorption 8.8 g/kg) were supplied by Infochems, South Korea. The silica (Z175MP, with the specific surface of 134.63 m^2/g and a mean particle size of 440 nm) was supplied by IDONG TECH.; silane coupling agent (Kettlitz-Silanogran Si69/GR) was supplied by Kangshin Industrial Co. Ltd.; aromatic oil (TDAE, dark brown, KUKDONG OIL & CHEMICAL CO. Ltd.) and maleic anhydride (MA) crystals (purity 99%, YONGSAN CHEMICALS INC) were supplied by IDONG TECH. The antiozonant (6PPD) and antioxidant (TMQ) and the rest of the curatives: zinc oxide (ZnO), stearic acid (SA), sulfur (S), tetramethylthiuram disulfide (TMTD), and N-cyclohexyl 2-benzothiazole sulfonamide (CZ) were all obtained from Infochems Company Ltd. The compound formulation expressed as parts per hundred parts of rubber (phr) with their respective codes is listed in Table 1.

2.2. Rubber Compounding Process. The rubber compounding was done in an internal mixer (model: QPBV-300, QMESYST, South Korea) at 90°C and 30 rpm. First, the elastomers were masticated in the kneader for 1 min, except for sulfur; the other processing ingredients were simultaneously added and mixed for about 2 min. Later, the reinforcements were incorporated and mixed for an additional of 1 min. Finally, the sulfur was added and then mixed for less than 30 seconds. The composition was passed over a two-roll mill (QM300, QMESYSTEM) repeatedly for about 9 min and then sheeted out. A rectangular sheet of samples (15 cm × 15 cm × 2 mm) was molded by electrical hot press machine (model: TO-200, TESTONE, South Korea) at a pressure of 25 tons with the help of the optimum curing conditions obtained from the cure rheometer (MDR, model: PDR2030, TESTONE Ltd., South Korea) at 160°C. The samples were cut into standard shapes and subjected to characterization analysis.

3. Characterization

3.1. Tensile Strength and Cyclic Loading. The tensile strength (TS) measurement for uncured and cured specimens was carried out according to ASTM D412 standard by using QM100s machine (QMESYSTEM, South Korea) at a crosshead speed of 500 mm/min and 25°C temperatures. For the uncured compositions, the maximum tensile stress was taken as the green strength from the generated stress-strain curve, and at least three samples were tested for each composition and averaged.

Table 1: Compound formulation and their codes measured in (phr)[a].

Chemicals	TP1	TP2	TP3	TP4	TP5	TP6	TP7	TP8
ENR	15	70	15	30	—	—	30	30
SBR	15	15	70	—	30	30	—	—
BR	70	15	15	70	70	70	70	70
ZnO	5	5	5	5	5	5	5	5
TMTD	1	1	1	1	1	1	1	1
CBS(CZ)	0.5	0.5	0.5	0.5	0.5	0.5	0.5	0.5
S/A	1.4	1.4	1.4	1.4	1.4	1.4	1.4	1.4
Sulfur	2.1	2.1	2.1	2.1	2.1	2.5	2.5	2.5
MA	3	3	3	3	3	—	3	3
N550	25	25	25	25	25	25	25	25
N330	10	10	10	10	10	10	—	10
TDAE	10	10	10	10	10	10	10	10
Silica	10	10	10	10	10	10	10	—
TESPT	3	3	3	3	3	3	3	—
TMQ	1.5	1.5	1.5	1.5	1.5	1.5	1.5	1.5
6PPD	1	1	1	1	1	1	1	1
Retarder	0.5	0.5	0.5	0.5	0.5	0.5	0.5	0.5
Wax	1	1	1	1	1	1	1	1

[a]Parts per hundred parts of rubber.

Table 2: Solubility parameters and calculated interaction parameters of solvent and polymers.

Samples/parameters	δ (cal/cc)$^{1/2}$	Estimated χ_1	Reference
*Toluene	8.91	—	[18]
*BR	8.38	0.352	[19]
*SSBR	8.04	0.372	[20]
*ENR	8.10	0.368	[21]

*Data for solubility parameters (δ) were taken from the corresponding literatures.

3.2. Peel Test (Tack Strength). The TS machine was used to carry out the peel test on the green samples. Sample preparation includes pressing the samples in between two mylar film for about 5 min. Prior to the test, the mylar film covering the faces of two rectangular samples strips (23 m × 65 mm × 2 mm) was removed and gently brought together. A pressure system of about 0.13 MPa was gently and uniformly applied on each side of the bonded strips at an equal rate. At least each press lasted for a contact time of about 10 seconds. The slight pressure given was to ensure interdiffusion and the removal of entrapped air bubbles at the interface of the bonded strips. Immediately after the pressing, the sample is subjected to the peel test. The peeling test was based on 180° orientation and at a speed of 50 mm/min. The tack strengths G_a (N/m) of the samples were then estimated. The testing machine generates plots of the force (Newtons) required to separate the bonded strips against the distance of separation (mm). The average forces required for separating bonded strips were recorded and together with the samples width, the G_a (N/m) was calculated using

$$G_a = \frac{2F}{d}, \tag{1}$$

where F is the estimated average peel force and d is the width (m) of the strips of the samples. For each composition, 3 samples were tested and averaged.

3.3. Crosslinking Density. Swelling experiments of cured composites were performed by equilibrating them in toluene at room temperature for 48 h. The swelling degree Q_r was calculated using the relation

$$Q_r = \frac{W_s - W_i}{W_d}, \tag{2}$$

where W_i is the weight of the rubber sample before immersion into the solvent; W_s and W_d are the weights of the sample in the swollen state and after drying in an oven at 80°C, respectively. The elastically active network chain density commonly referred to as the crosslink density N was calculated from the Flory-Rehner equation given by equation (3) [16]

$$-\left[\mathrm{In}(1-v_r) + v_r + \chi_1 v^2{}_r\right] = v_s \left[\frac{v_r{}^{1/3} - v_r}{2}\right] N, \tag{3}$$

where $v_r(1/Qr)$ is the volume fraction of polymer in the swollen gel at equilibrium, v_s is the molar volume of the solvent (106.3 mL/mol for toluene), and χ_1 is the polymer-solvent parameter determined from Bristow-Watson equation (4) [17], where

$$\chi_1 = \beta_1 + \left(\frac{v_s}{RT}\right)\left[\delta_s - \delta_p\right]^2, \tag{4}$$

where β is the lattice constant, usually taken as 0.34, v_s is the molar volume of solvent, R is the universal gas constant, T is the absolute temperature, and δ is the solubility parameter, and the subscripts s and p refer to the swelling agent and polymer, respectively. The solubility parameters (δ) with respective estimated interaction parameters (χ_1) of BR, SBR, ENR, and solvent (toluene) are as shown in Table 2.

3.4. Abrasion Resistance. The abrasiveness of the various composites was examined by using the DIN abrasion instrument obtained from QMESYS Co. Ltd. A cylindrical-like rubber test specimen (~6 mm thickness) was made and abraded against an abrasive surface mounted on a rotating cylindrical drum. The amount of rubber reduced in the specimen due to abrasion is measured. At least, three samples were tested and averaged for one composition.

3.5. Fatigue Behavior. The flex-fatigue life of various compounds was measured using a De Mattia flexing machine (QM 650D) according to ASTM D430 [22]. The specimen shapes and dimensions are shown in Figure 2). The specimen thickness was measured close to the groove. The conditions used include conditioning the test specimens for at least 12 h at the test temperature of 23 ± 1°C and doing the test at a 300 ± 10 cycles/min. For each composite, three pieces were

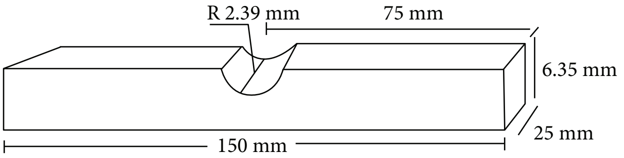

Figure 2: De Mattia flexing specimen with a semicircular groove that was used to measure the flex-fatigue life of the various samples [22].

tested, and the average flex-fatigue-life value was reported. The flex-fatigue life was defined by the cycles at which a visible crack (a grade-one crack) was observed.

3.6. Resilience. The resilience of the various compounds was tested by using DIN resilience tester (DIN 53512 and ISO 4662) obtained from QMESYS Company Ltd. The hammer of the instrument was allowed to strike the samples (~6 mm thickness) for about 5 times to eliminate internal defects; the values of the remaining hits were recorded. Three samples were tested for each composition; and their results were averaged.

3.7. Hardness Test (Shore A). A constant loader hardness tester (Shore A) with a load of 5 kg was used to test the hardness of the vulcanizates. At least 3 samples of about ~5 mm thickness were tested and averaged for one composition.

4. Results and Discussions

4.1. Green and Tack Strength. In the tire manufacturing technology, the various uncured components of the tire are brought together and gently assembled before vulcanization begins in the curing chamber; hence, self-adhesion (similar interface), adhesive tack (dissimilar interface), and green strength of the rubber compounds intended for industrial tire tread development are the crucial part of the tire/tread design. Here, we present the green strength (GS) and self-adhesion properties of the various tread-based compounds as shown in Figures 3(a) and 3(b). The samples labeled TP2 and TP4 showed inferior GS probably due to higher stiffness as a result of strong interactions (rubber-filler or filler-filler), especially with blends rich in ENR. The compounds with relatively higher stiffness such as sample TP2 have indicated inferior tack strength (see Figure 3(b)), which is related to the inability of the rubber molecules to flow or interdiffuse across the interface. Although sample TP7 contains 30 phr ENR, with only one carbon black (CB), N550 and silanized silica (Si) showed higher green strength compared to TP2 (70 phr ENR) with triple-filler mixtures and others. Also, the sample without silica (TP8) shows improved GS than the one with silanized silica inclusion (TP4). These observations could mean that the combination of a two-filler system (N550 and silanized silica) offers effective reinforcing action in low ENR compounds than the three-phase filler systems, probably due to extreme inhomogeneity. Also, the GS has improved for TP5 (with MA) than TP6 (without MA), indicating that MA induced a grafting process during the melt blending stage. When the GS and tack strength of all the compounds are compared, it can be observed that compositions enriched with high content of the low glass transition temperature (T_g) elastomers (BR and SBR) shows somewhat better GS and tack strength than those enrich in ENR. This is because the molecular movement of the low T_g molecules is higher, although the filler inclusion restricts the mobility of their chains. However, the average depth of penetration of the interdiffused chains was still adequate to form entanglement on either side of the interface (Figure 3(c)) and thus offered greater resistance to peeling compared to compounds enriched with ENR which appears to have obtained higher reinforcement effect. Thus, the current compounds have exhibited higher GS than isobutylene-isoprene gum-montmorillonite loaded BIIR-MMT (0~16 phr) composites [23], probably due to high reinforcements. Additionally, BIIR-MMT compounds also show higher GS and tack strength than the current compounds, owing to lower T_g and lower elasticity characteristics nature of BIIR gum [23, 24].

4.2. Rheometry Properties. The curing properties which include onset and optimum curing time (t_{s2} and T_{90}), the minimum and maximum torque (M_L and M_H), the differences in torque ($\Delta M = M_H - M_L$), and the cure rate index (CRI) ($100/(T_{90}\text{-}t_{s2})$), of the various compounds deduced from the rheo-curves at 160°C are plotted in Figures 4(a)–4(d). When the blend gets richer in SBR, there is an increase in the T_{90} due to possible diffusion of curatives from SBR interface to ENR and/or BR interface as illustrated in Figures 5(a) and 5(b), suggesting higher crosslinking density accumulation at these phases [25]. Also, the presence of the MA was found to cause further delaying in T_{90}. For example, when MA was excluded from the blend (i.e., TP6), the T_{90} dropped drastically with higher cure rate compared to its counterpart (TP5 with MA) and the rest of the composition containing MA, as seen in Figures 4(a) and 4(b). Although the MA is supposed to play a role of compatibilizer and grafting within the blends (example: ENR-MA-g-ENR, ENR-g-MA-BR, ENR-g-SBR, and BR-g-MA-SBR), the anhydrides groups on MA have acted as scavengers of free radicals and consequently retarded vulcanization of the compounds.

It is interesting to also observe that removal of the silanized silica from the composition (i.e., TP8) slightly minimized the T_{90}, suggesting that silanized silica took part in the curing reaction.

A similar trend was observed when NR was filled with silanized silica; the t_{s2} and T_{90} has shortened [26]. The t_{s2} of TP2, TP5, and TP7 has slightly dropped compared to the other blends. The TP2 and TP7, respectively, contain 70 phr and 30 phr of ENR in the blends with epoxide groups that might have participated in the initial vulcanization reaction of the blends. Nelson and Kutty [27], after grafting MA to a whole tire, reclaim that both t_{s2} and T_{90} is delayed. The TP2 ENR (70 phr) reveal the highest M_L(viscosity index), M_H (crosslinking density index), and consequently ΔM (strength index) compared to those with a lower content of ENR as well as other blends. This observation has confirmed the possible diffusion of curatives from SBR phase to the ENR phase with higher crosslinking density which is also observed by Goyanes et al. [25].

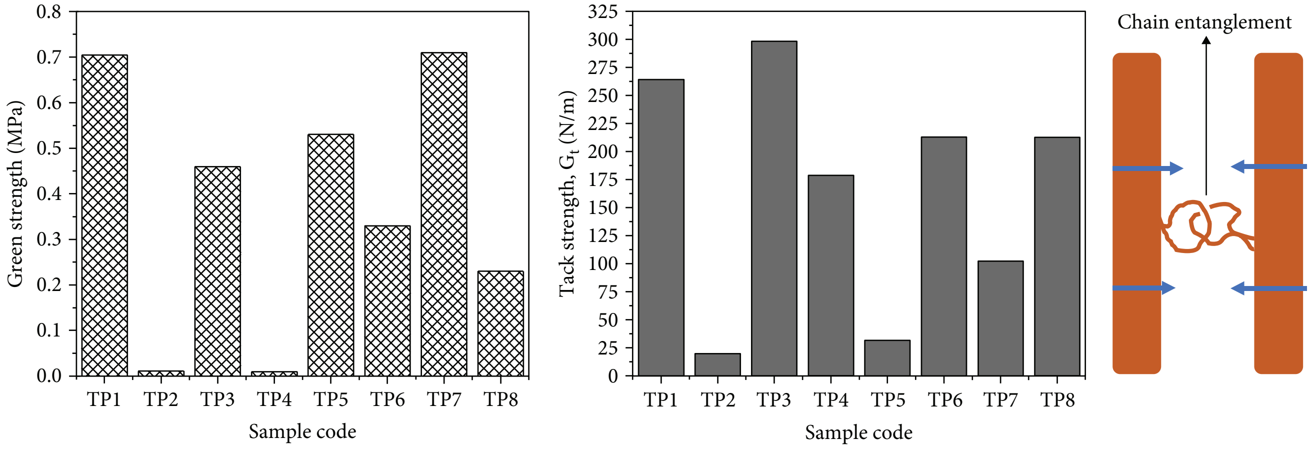

(a) (b) (c)

FIGURE 3: Green strength and autohesion behavior of uncured composites.

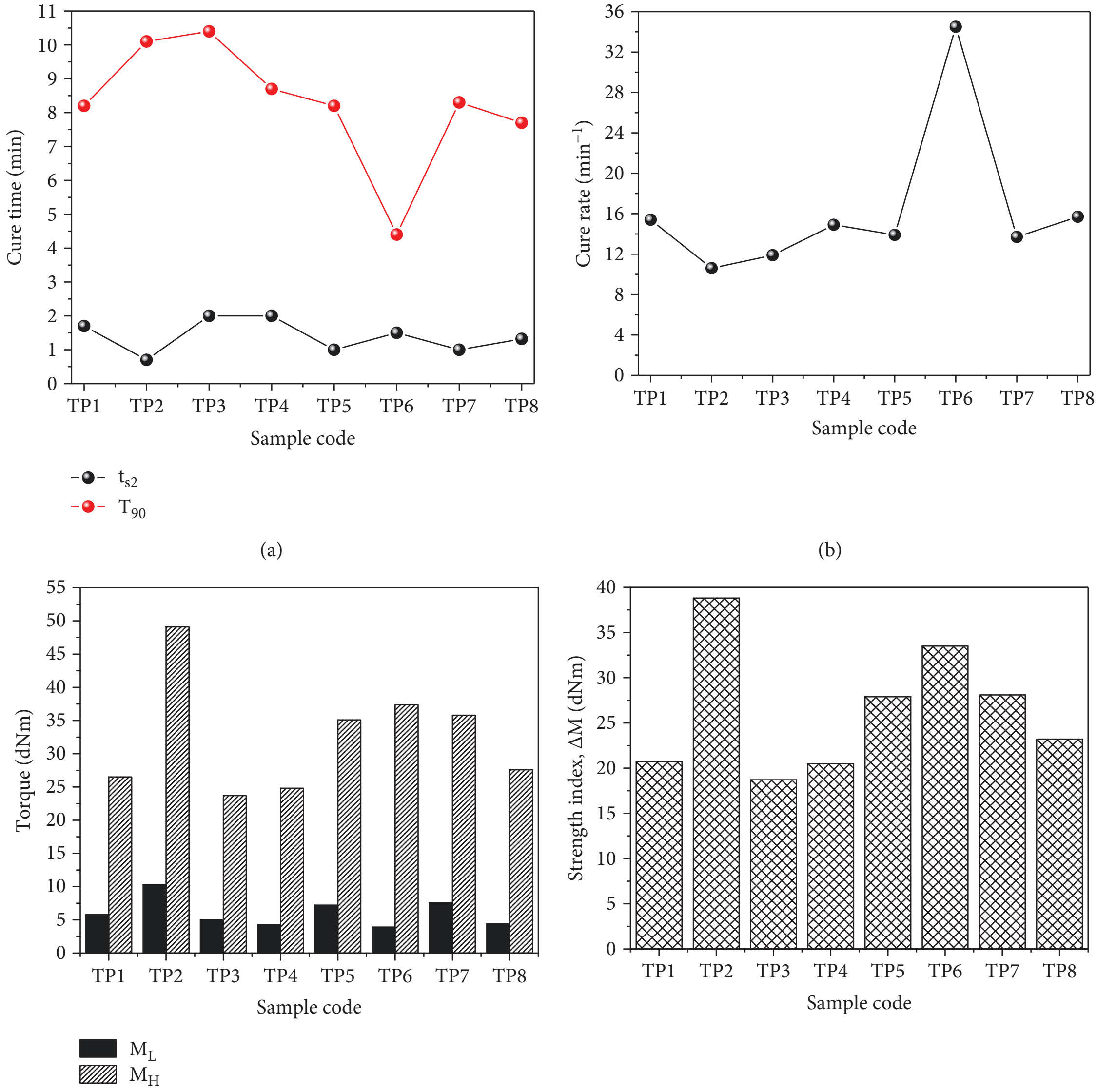

(a) (b)

(c) (d)

FIGURE 4: Rheometry properties of the various compounds cured at 160°C.

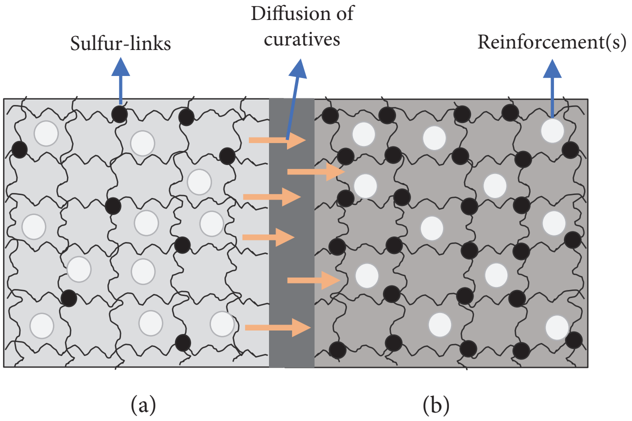

Figure 5: Illustration of interfacial diffusion of curatives from ENR-SBR or ENR-BR interface to ENR phase; (a) phase of SBR and (b) phase of ENR.

It is also interesting to know that the TP7 (only one CB) and TP8 (without silica) have improved torques (M_H and ΔM) than their counterpart blend TP4 (30 phr ENR, 70 phr BR with mixtures of CB and silanized silica). This can mean that a combination of the three fillers has not favored TP4 blend formation.

In general, the curing properties of the present tread-based compounds have exhibited better performances than those reported earlier for NR (75 phr)/BR (25 phr)-CB (50 phr)/silica (10 phr), NR (75 phr)/BR (25 phr)-CB (60 phr) [5] and NR-CB (53 phr), and NR (80 phr)/SBR (20 phr)-CB (57 phr) [6]. Also, the proposed passenger tire tread compounds by Atashi and Shiva [7] show severe delays in curing (t_{s2} and T_{90}) compared to our current development. Again, when ENR was used as a compatibilizer in NR at varying amounts (5–20 phr), lengthening of curing times; t_{s2}: 4~11 min and T_{90}: 9~19 mins were recorded compared to our current work. It was assumed that the silica (Si) adsorbed the curing accelerator onto its surface as silanol which underwent hydrogen bonding with silanol groups [14]. However, it should be emphasized here that properties like M_H and ΔM may not be subject to only chemical networks creation but also physical networks are possible; hence, further tests are presented to further examine physico-mechanical properties of the various vulcanizates.

4.3. Crosslinking Density. The degree of swelling of polymer composites in the desired solvent has been a useful technique to check the matrix-filler interaction of composites. For composites with one matrix system, only the calculated interaction parameter (χ_1) of that matrix is used in the estimation of its crosslinking density (N) [28, 29]. Researchers have adopted the use of the mixtures rule [30] for blend systems or a method of averaging χ_1 for each the polymer involved to compute the N of composites with many matrix phases [18, 20, 31]. In this present study, we also adopted the latter method of averaging χ_1 for the blend systems, for the computation of their respective N values. The results of equilibrium swelling ratio (Q_r), the calculated solubility parameters (δ), the interaction parameters as well as their respective crosslinking densities (N) for the blends are as presented in Table 3.

Table 3: Swelling properties and crosslinking densities of the various compounds.

Samples/parameters	Q_r	δ (cal/cc)$^{1/2}$	χ_1	N (mol/cm^3)
TP1	1.736	8.173	0.363	0.00412
TP2	1.059	8.173	0.363	0.02997
TP3	1.590	8.173	0.363	0.00378
TP4	2.290	8.070	0.370	0.00116
TP5	1.418	8.210	0.361	0.00588
TP6	1.569	8.210	0.361	0.00399
TP7	1.609	8.240	0.359	0.00366
TP8	1.792	8.240	0.359	0.00253

The TP2, a triple matrix composites of SBR: 15 phr, BR: 15 phr, and ENR: 70 phr, has shown the least Q_r with corresponding thrilling N value, indicating a stronger interaction (filler-polymer and/or filler-filler) in comparison with the remaining samples. During the vulcanization process, the sulfur could form bridges between the organic tail of silanized silica and the backbone of ENR (see Figure 6i), whilst the carbon blacks and the ENR can also provide additional hydrogen bonding via polar-polar interactions (see Figure 6ii). Thus, the crosslinking reaction seems to favor the blends with richer ENR leading to an increase N. The next sample with the highest N is TP5, and the order TP5 > TP6 and TP5 > TP8 suggests that MA and silanized silica play an effective role in the crosslinking reaction. The blend with mixtures of only N550 and silanized silica (TP7) attains comparable N as TP5 (30 phr SBR/70 phr BR), but TP4 attains the poorest N behavior although it contains 30 phr ENR with mixtures of carbon blacks and silanized silica.

This observation can be ascribed to the possible formation of agglomerates which dominates the filler-polymer interactions. Although the changes in the δ and their corresponding χ_1 for a mono, dual, and triple matrix system could influence the N values of the corresponding compounds; however, the pattern of variation of N for the various blend systems in this present work has still remained unaffected. The influence of N on the remaining physico-mechanical properties of the various compounds is presented in the proceeding sections.

4.4. Tensile Properties and Hardness. The tensile properties which include tensile strength (MPa), elongation at break (%), modulus at 200 and 300% (M200 and M300), and the Young's modulus (MPa) deduced at lower strain less than 5% of the various blends are presented in Figures 7(a)–7(d). The order of decreasing tensile strength is TP5 > TP1 > TP3 > TP6 > TP7 = TP4 > TP2 > TP8, with TP5 (30 phr SBR/70 phr BR) being the highest and TP8 (without silica) the least. It can be observed that the blends richer in BR and/or SBR seem to show higher tensile strength (see Figure 7(a)) and elongation at break (see Figure 7(b)) compared to the blends rich in ENR. This is because the high crosslink density in the ENR-based systems (refer to Figure 4 and Table 3)

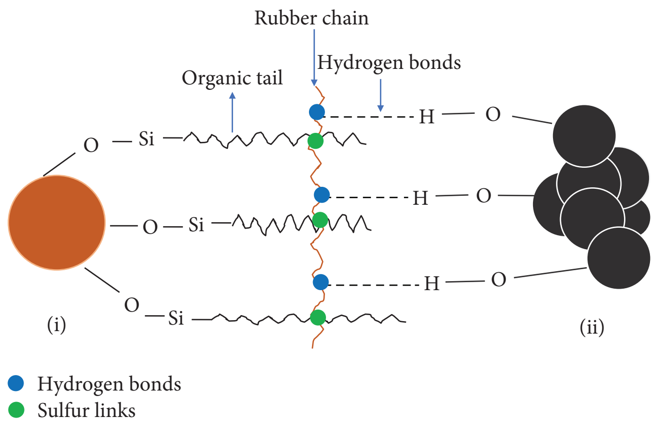

Figure 6: Illustration of possible bond formations between silanized silica, carbon blacks, and rubber molecules.

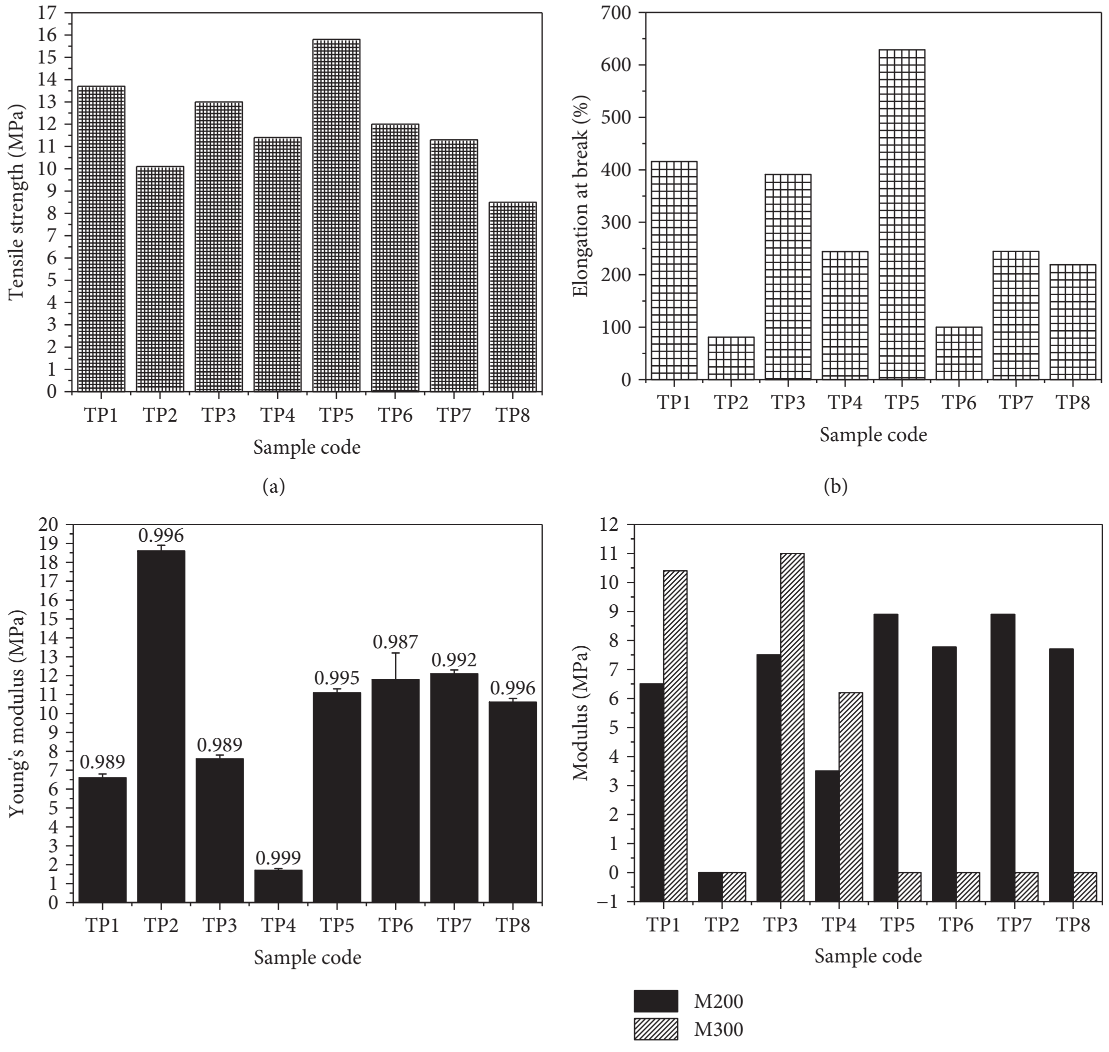

(a)

(b)

(c)

(d)

Figure 7: Tensile properties of vulcanizates: (a) tensile strengths, (b) modulus at 300 and 200%, (c) Young's modulus at strain less than 10%, and (d) elongation at break.

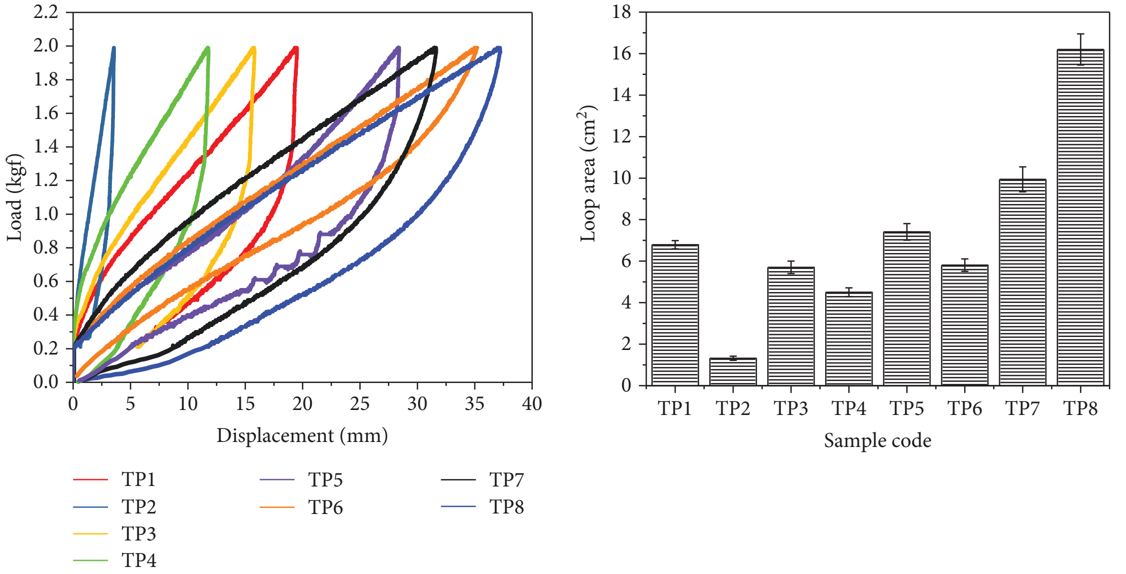

(a)

(b)

Figure 8: Cyclic testing of the vulcanizates; (a) the first loop after first cycles of vulcanizates and (b) area of the loop of the first cycle.

have made them much rigid and less stretchable (brittle-like) than the others (see Figures 7(c) and 7(d)).

Additionally, the T_g of virgin ENR is generally higher due to the epoxide functionalities (T_g dependent on epoxide content) [32, 33] and appears to increase further upon filler inclusion (becomes stiffer) compared to the low T_g elastomers (BR and SBR) [34] of the same filler loading. One observation is that the inclusion of silanized silica to the blends promotes filler-polymer interaction resulting in improved tensile strength, suggesting the 35% increment in tensile strength in TP4 (30 phr ENR/70 phr BR) which contains 10 phr of silanized silica more than its counterpart TP8 (30 phr ENR/70 phr BR) without silica. It can also be observed that the inclusion of MA contributes to higher tensile strength, a reason why TP5 (30 phr SBR/70 phr BR) with MA has obtained more than 33% growth in tensile strength than TP6 (30 phr SBR/70 phr BR) of the same filler loading but without MA. Meanwhile, the tensile strength is not much affected when only one type of CB is used (in the case of TP7) compared to those with two mixtures of CBs (TP4). The tensile properties of this present compounds have generally improved compared to the truck-based tread compounds comprising of NR (75 phr)/BR (25 phr)-CB (50 phr)/Si (10 phr) and NR (75 phr)/BR (25 phr)-CB (60 phr) proposed earlier by Zafarmehrabian et al. [5].

4.5. Hysteresis Loss. The viscoelastic behavior of elastomer results in an energy loss during a cycle of extension-contraction; the energy loss is called hysteresis (or hysteretic loss). The hysteresis loss is related to the rolling resistance (RR) (fuel consumption) of tread tire; the higher the hysteresis loss, the higher the RR of a moving tire and the higher fuel is consumed [35]. The cyclic loading is indicated in stress-strain plots in Figure 8(a) whilst the area of loss is plotted in Figure 8(b). The decreasing order of the hysteresis loss is due to the estimated area of cyclic curves of the various blends and it decreases in the order: TP2 > TP4 > (TP3 = TP6) > TP1 > TP5 > TP7 > TP8. As shown, compounds rich in ENR content containing the three mixtures of fillers (N550, N330, and silanized silica) have indicated lower areas associated with improvement in hysteresis loss. Next is the compound with a high content of SBR and/or BR blend ratio containing all the mixture of fillers.

Blends with only one CB (25 phr of N550) with silanized silica (10 phr) do not contribute to the improvement in hysteresis compared to those with triple filler mixtures. For instance, TP7 (30 phr ENR/70 phr SBR) with 25 phr (N550) and silanized silica (10 phr) is 133% higher (poor RR effect) compared to TP4 (30 phr ENR/70 phr SBR) with mixtures of CBs (25 phr N550/10 phr N330) and silanized silica (10 phr). This means that complementary of the fillers enhances hysteresis loss, even though the formation and collapsing of aggregate (filler-filler accumulation) which leads to frictional energy is possible [35]. Nonetheless, it appears the TP4 (30 phr ENR/70 phr SBR) contributes more to the improvement in hysteresis loss compared to compounds without silica (TP8) which attains extremely high loop area (higher hysteresis loss) of about 277%. Therefore, it has been seen that lower hysteresis loss (lower RR) is consistent with the compounds with higher stiffness.

4.6. Hardness and Wear Resistance. Figures 9(a) and 9(b) represent the hardness and abrasion loss (mg) of the various blends. Again, the compound with higher crosslinking density (N) and Young's modulus with improved hysteresis loss (TP2) has attained higher hardness properties whilst TP4 showed the least. According to Zafarmehrabian et al. [5], abrasion behavior of rubbers is influenced by two crucial factors: modulus and N. That is, high modulus and N lead to the enhancement of the abrasion strength of rubber compounds [5]. Contrary, the blend TP2 (with high ENR content) attained the inferior abrasion resistance (see Figure 9(b))

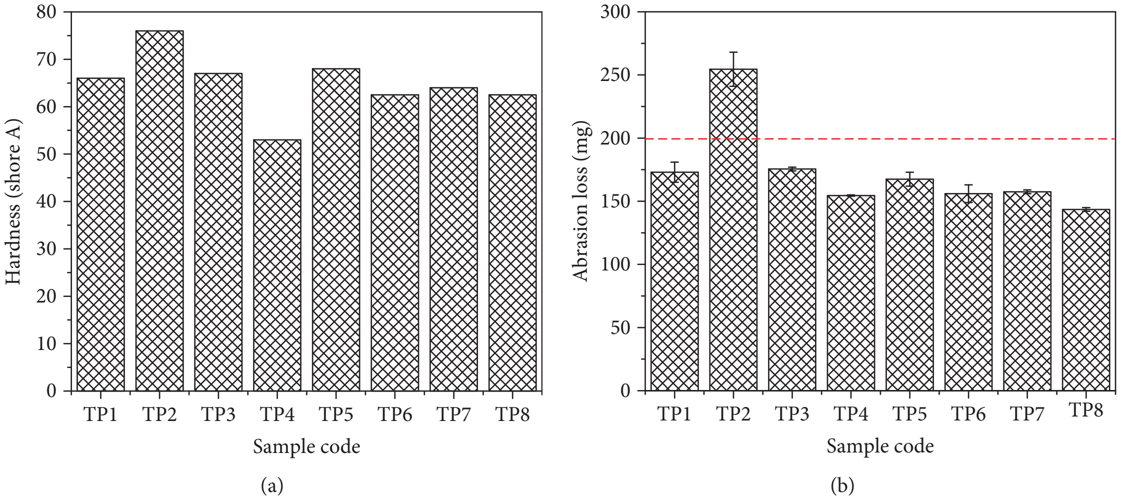

(a)

(b)

Figure 9: Hardness and wear resistance of the vulcanizates.

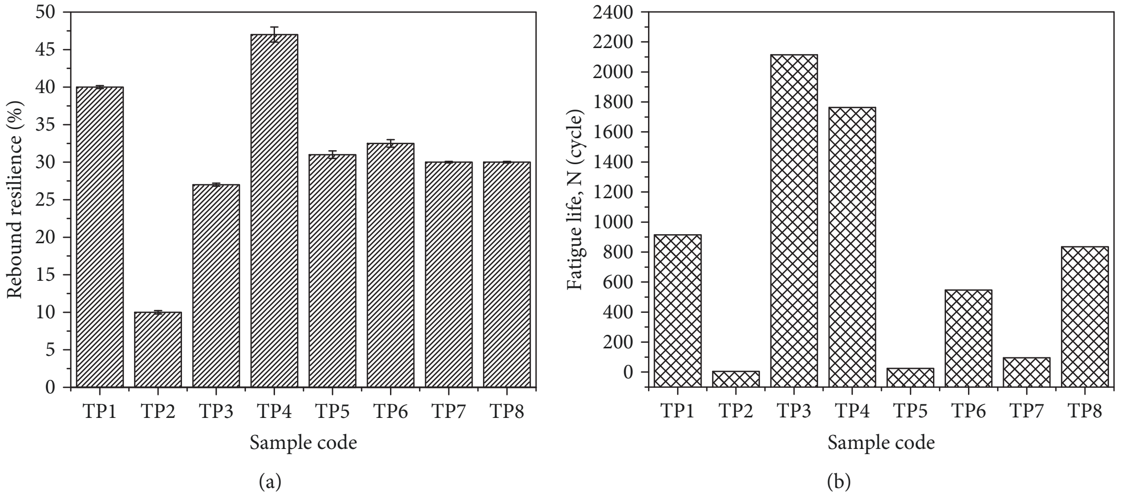

(a)

(b)

Figure 10: Rebound resilience and fatigue fracture properties of vulcanizates.

compared to the remaining samples which have shown relatively lower abrasion loss (improved wear resistance). The abrasion loss of these compounds is less than 200 mg (mass loss), a prerequisite for tire treads, shoe soles, and other abrasive surfaces. The inclusion of silanized silica was reported to improve the wear of rubber compounds due to strong filler-rubber interactions [7]. However, in this work, the compound without silica showed relatively improved wear resistance compared to those containing silica. Thus, it can be concluded that a critical level of modulus and *N* are required to promote improved wear resistance. Therefore, an improvement in wear resistance must be explained in terms of the nature of network density such as filler-filler and/or filler-rubber and degree of *N*.

4.7. Resilience and Fatigue Properties. The resilience and fatigue properties of the various tread compounds are shown in Figures 10(a) and 10(b). The resilience seems to be dependent on the three factors: stiffness, hardness, and crosslinking density (*N*). The higher these properties, the lower the resilience; hence, TP2 (with extremely high *N*, hardness, and stiffness) shows the least resilience property. Another observation is that the resilience of the compounds seems to have been improved with compounds rich in BR content and less amount of ENR and/or SBR phases as in TP4 (30 phr ENR/70 phr BR) and TP1 (15 phr ENR/15 phr SBR/70 phr BR). This is because BR is well known for its higher resilience (the ability to recover size and shape after stress) compared to NR and SBR elastomers [36]. Generally, we have observed that the compounds TP1 and TP4 have shown higher resilience properties than the industrial tread compounds (80 phr NR/20 phr SBR/57 phr N375): 38.9%, (80 phr NR/20 phr SBR/57 phr N339): 38.4%, and (72 phr NR/28 phr SBR/55 phr N339): 34.5% reported earlier by Bijarimi et al. [6]. Also, apart from the rigid tread compound (TP2), the current compounds have still exhibited higher resilience properties than those reported for the blend (60 phr SBR/20 phr BR/20 phr NR/50 phr of N324), which obtained 20% as the sample with the best resilience properties by Atashi and Shiva et al. [7]. Furthermore, the fatigue

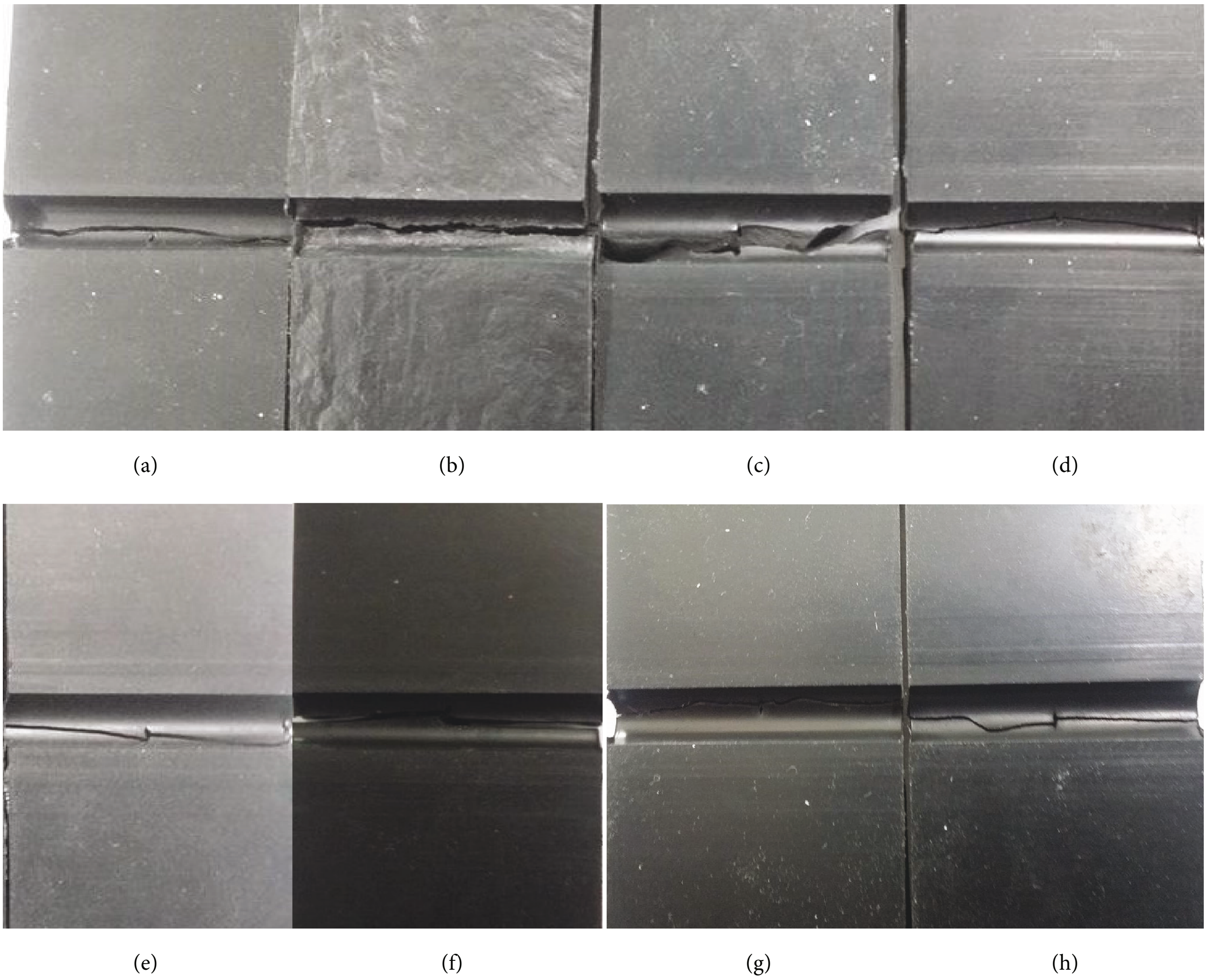

Figure 11: Morphology and mechanism of fatigue fracture of various vulcanizates; (a) TP1, (b) TP2, (c) TP3, (d) TP4, (e) TP5, (f) TP6, (g) TP7, and (h) TP8.

life which is generally related to the crack-growth characteristics of rubber materials has been presented in Figure 10(b).

The order of reducing in fatigue life is TP3 > TP4 > TP1 > TP8 > TP6 > TP7 > TP2 = TP5. The styrene content of the SBR sample has been observed to hinder the rotation of the backbone of SBR and also makes the backbone rigid [36]. Hence, high viscoelastic energy dissipation during the stretching and collapsing of the rigid structure of SBR may have introduced strain-induced crystallization that retards its failure. Again, it appears compounds with a high content of ENR and lower SBR phases show inferior fatigue properties due to extreme rigidity of bonds or higher networked density of the samples (TP2, TP5, and TP7). With the increased crosslinking density (N), the gel point of the blends is reached, and fatigue fracture (breaking of chemical bonds) becomes eminent. Thus, compounds with low molecular weight and substantial number of free-chain ends associated with large viscous flow portions such as TP3 (15 phr ENR/70 phr SBR/15 phr BR), TP4 (30 phr ENR/70 phr SSBR/25 phr N550/10 phr N330/10 phr silanized silica), and TP1 (15 phr ENR/15 phr SBR/70 phr BR/25 phr N550/10 phr N330/10 phr silanized silica) demonstrated the highest fatigue property compared to the compounds with restricted mobility of chains. When observed, TP4 (with silanized silica) is over 117% higher in fatigue resistance than its counterpart of the same composition except without silanized silica. This indicates an additional reinforcement offered by the silanized silica. Also, next sample which attained good fatigue property is TP8 (without silica). When the compound TP7 is compared with TP4 and TP8 of the same compositions except for only one carbon black filler and silanized silica, it is obvious that the high surface area carbon black does not enhance fatigue properties at this loading level as low surface area carbon black will do, because it is reported that as the surface area of carbon black increases, the maximum fatigue resistance shifts towards lower filler loading [36, 37]. Another observation is that when the MA was eliminated from the compounds (in the case of TP6), it has attained over 2000% increment in fatigue resistance compared to the compound of the same composition without MA, confirming that MA contributed to the formation of tightly crosslinks structures (filler-rubber links). The mode of fatigue of the various compounds has been discussed in the next sections for better understanding.

4.7.1. Mechanism of Fatigue Failure of Composites. The fracture mechanism and process can be viewed and analyzed physically by using microscopic techniques such as SEM, TEM, and AFM to analyze the morphology of suspicious vulcanizates. Here, we present a photo of the cracked surface of the various blends as presented in Figures 11(a)–11(h). In general, some samples (with higher crosslinking densities) such as TP2, TP5, and TP7 show a kind of stable brittle-like crack path associated with the low fatigue resistance (order of decreasing inferiority: TP2 > TP5 > TP7). Also, TP2 with the superior crosslinking density demonstrates a rocky-like surface, indicating a brittle-like behavior. Meanwhile, the remaining samples with relatively low crosslinking densities (TP1, TP3, TP4, TP6, and TP8) exhibit a kind of unstable brittle-like fracture paths, with somewhat high failure resistance when compared. In particular, the sample TP3 (Figure 11(c)) has exhibited a kind of nonunidirectional crack propagation path popularly called knotty crack growth, a mechanism linked to redistribution of loads by either crystalline sites in the composites or well aligned reinforcements, thereby reducing the sudden failure of the bulk matrix [35, 38]. This could explain why TP3 exhibited high fatigue strength in relation to its counterparts.

5. Conclusions

Various rubber blends filled with carbon black mixtures and silanized silica were prepared by melt mixing process and their various physico-mechanical properties examined for the suitability of tread applications. It was observed that high content of ENR (~70 phr) greatly improves the crosslinking density, Young's modulus, and hysteresis loss (lower rolling resistance), and at the same time, poor abrasion resistance and fatigue failure properties are obtained. Although it is challenging to obtain all the properties for green tire (WT, RR, and WR) at some instance due to compromising effects of properties, however, adopting blends with small amount of ENR content such as TP4 (30 phr ENR/70 phr SBR) with mixtures of CBs (25 phr N550/10 phr N330) and silanized silica (10 phr) present a suitable composition for developing tread with fuel-saving capabilities can be achieved.

Data Availability

The authors confirm that all the data used in this work has been provided in the text. And that there are no restrictions or whatsoever to the use of the data in the text for scientific or commercial purposes. Any request could be directed to the corresponding author's email: ayaya@ug.edu.gh.

Conflicts of Interest

The authors declare that they have no conflicts of interest.

Acknowledgments

A. Yaya acknowledges the financial support from the University of Ghana Building a New Generation of Academics in Africa (BANGA-Africa) Project, with funding from the Carnegie Corporation of New York. The assistance offered by YUTECH Company (South Korea) for granting us access to use their facilities for this work is also acknowledged.

References

[1] S. H. Cadle and R. L. Williams, "Gas and particle emissions from automobile tires in laboratory and field studies," *Journal of the Air Pollution Control Association*, vol. 28, no. 5, pp. 502–507, 1978.

[2] D. J. Schuring, "Effect of tire rolling loss on vehicle fuel consumption," *Tire Science and Technology*, vol. 22, no. 3, pp. 148–161, 1994.

[3] A. Y. C. Lou, "Relationship of tire rolling resistance to the viscoelastic properties of the tread rubber," *Tire Science and Technology*, vol. 6, no. 3, pp. 176–188, 1978.

[4] T. Freudenmann, H.-J. Unrau, and M. El-Haji, "Experimental determination of the effect of the surface curvature on rolling resistance measurements," *Tire Science and Technology*, vol. 37, no. 4, pp. 254–278, 2009.

[5] R. Zafarmehrabian, S. T. Gangali, M. H. R. Ghoreishy, and M. Davallu, "The effects of silica/carbon black ratio on the dynamic properties of the tread compounds in truck tires," *Journal of Chemistry*, vol. 9, no. 3, p. 1112, 2012.

[6] M. Bijarimi, H. Zulkafli, and M. D. H. Beg, "Mechanical properties of industrial tyre rubber compounds," *Journal of Applied Sciences*, vol. 10, no. 13, pp. 1345–1348, 2010.

[7] H. Atashi and M. Shiva, "Formulation for passenger tread tire compound based on styrene butadiene rubber/cis-butadiene rubber/natural rubber blend and semi-dispersible silica/carbon black filler system," *Asian Journal of Chemistry*, vol. 22, pp. 7519–7530, 2010.

[8] G. Kraus and H. R. Hunt, "Carbon black for low-hysteresis rubber compositions," 1978, Google Patents.

[9] W. K. Dierkes, L. A. Reuvekamp, A. J. Ten Brinke, and J. W. Noordermeer, *Silanes and Other Coupling Agents*, vol. 3, p. 89, 2004.

[10] G. J. Lake, "Ozone cracking and protection of rubber," *Rubber Chemistry and Technology*, vol. 43, no. 5, pp. 1230–1254, 1970.

[11] Y. Okado, M. Kawamura, and T. Tomioka, "Rubber composition comprising furnace carbon black," 1982, Google Patents.

[12] S. S. Sarkawi, A. K. C. Aziz, R. A. Rahim, R. A. Ghani, and A. N. Kamaruddin, "Properties of epoxidized natural rubber tread compound: the hybrid reinforcing effect of silica and silane system," *Polymers & Polymer Composites*, vol. 24, p. 775, 2016.

[13] W. Kaewsakul, K. Sahakaro, W. K. Dierkes, and J. W. Noordermeer, "Verification of interactions between silica and epoxidised squalene as a model for epoxidised natural rubber," *Journal of Rubber Research*, vol. 17, p. 129, 2014.

[14] K. Sengloyluan, K. Sahakaro, and J. W. Noordermeer, "Use of epoxidized natural rubber as a compatibilizer in silica-filled natural rubber compounds," in *28th International Conference of the Polymer Processing Society 2012*, Nuremberg, Germany, 2012.

[15] P. J. Martin, P. Brown, A. V. Chapman, and S. Cook, "Silica-reinforced epoxidized natural rubber tire treads — performance and durability," *Rubber Chemistry and Technology*, vol. 88, no. 3, pp. 390–411, 2015.

[16] P. J. Flory and J. Rehner Jr, "Statistical mechanics of cross-linked polymer networks I. rubberlike elasticity," *The Journal of Chemical Physics*, vol. 11, no. 11, pp. 512–520, 1943.

[17] G. M. Bristow and W. F. Watson, "Cohesive energy densities of polymers. Part 1.—Cohesive energy densities of rubbers by swelling measurements," *Transactions of the Faraday Society*, vol. 54, pp. 1731–1741, 1958.

[18] B. Moon, J. Lee, S. Park, and C.-S. Seok, "Study on the aging behavior of natural rubber/butadiene rubber (NR/BR) blends using a parallel spring model," *Polymer*, vol. 10, no. 6, p. 658, 2018.

[19] B. A. Miller-Chou and J. L. Koenig, "A review of polymer dissolution," *Progress in Polymer Science*, vol. 28, no. 8, pp. 1223–1270, 2003.

[20] S. El-Sabbagh and A. Yehia, "Detection of crosslink density by different methods for natural rubber blended with SBR and NBR," *Egyptian Journal of Solids*, vol. 30, p. 157, 2007.

[21] J. B. Nagode and C. M. Roland, "Miscible mixtures of polychloroprene and epoxidized polyisoprene," *Polymer*, vol. 32, no. 3, pp. 505–509, 1991.

[22] Y. P. Wu, W. Zhao, and L. Q. Zhang, "Improvement of flex-fatigue life of carbon-black-filled styrene-butadiene rubber by addition of nanodispersed clay," *Macromolecular Materials and Engineering*, vol. 291, no. 8, pp. 944–949, 2006.

[23] B. Mensah, S. Kim, D. H. Lee, H. G. Kim, J. G. Oh, and C. Nah, "Autohesion behavior of brominated-isobutylene-isoprene gum nanocomposites with layered clay," *Elastomers and Composites*, vol. 49, no. 1, pp. 43–52, 2014.

[24] K. Chino, M. Ashiura, J. Natori, M. Ikawa, and T. Kawazura, "Thermoreversible crosslinking rubber using supramolecular hydrogen bonding networks," *Rubber Chemistry and Technology*, vol. 75, no. 4, pp. 713–723, 2002.

[25] S. Goyanes, C. C. Lopez, G. H. Rubiolo, F. Quasso, and A. J. Marzocca, "Thermal properties in cured natural rubber/styrene butadiene rubber blends," *European Polymer Journal*, vol. 44, no. 5, pp. 1525–1534, 2008.

[26] S. S. Idrus, H. Ismail, and S. Palaniandy, "The effects of silanized ultrafine silica on the curing characteristics, tensile properties, and morphological study of natural rubber compounds," *Polymer-Plastics Technology and Engineering*, vol. 50, no. 1, pp. 1–7, 2011.

[27] P. Nelson and S. Kutty, "Studies on the utilisation of rubber reclaim in elastomers," *Progress in Rubber Plastics and Recycling Technology*, vol. 19, p. 171, 2003.

[28] B. Mensah, S. Kim, S. Arepalli, and C. Nah, "A study of graphene oxide-reinforced rubber nanocomposite," *Journal of Applied Polymer Science*, vol. 131, no. 16, 2014.

[29] C. Nah, S. G. Kim, G. S. Shibulal et al., "Effects of curing systems on the mechanical and chemical ageing resistance properties of gasket compounds based on ethylene-propylene-diene-termonomer rubber in a simulated fuel cell environment," *International Journal of Hydrogen Energy*, vol. 40, no. 33, pp. 10627–10635, 2015.

[30] M. A. Mansilla, L. Silva, W. Salgueiro, A. J. Marzocca, and A. Somoza, "A study about the structure of vulcanized natural rubber/styrene butadiene rubber blends and the glass transition behavior," *Journal of Applied Polymer Science*, vol. 125, no. 2, pp. 992–999, 2012.

[31] H. S. Ahmad, H. Ismail, and A. Abd. Rashid, "ENR-50 compatibilized natural rubber/recycled acrylonitrile-butadiene rubber blends," *Sains Malaysiana*, vol. 44, no. 6, pp. 835–842, 2015.

[32] V. Tanrattanakul, B. Wattanathai, A. Tiangjunya, and P. Muhamud, "*In situ* epoxidized natural rubber: improved oil resistance of natural rubber," *Journal of Applied Polymer Science*, vol. 90, no. 1, pp. 261–269, 2003.

[33] N. A. Kinasih, M. I. Fathurrohman, and D. A. Winarto, "Swelling behaviour in n-pentane and mechanical properties of epoxidized natural rubber with different epoxide content," *IOP Conference Series: Materials Science and Engineering*, vol. 223, article 012002, 2017.

[34] W. M. Groenewoud, *Characterisation of Polymers by Thermal Analysis*, Elsevier Science, 2001.

[35] J. de Castro, R. Zargar, M. Habibi et al., "Nonmonotonic fracture behavior of polymer nanocomposites," *Applied Physics Letters*, vol. 106, article 221904, no. 22, 2015.

[36] J. Zhao and G. N. Ghebremeskel, "A review of some of the factors affecting fracture and fatigue in sbr and br vulcanizates," *Rubber Chemistry and Technology*, vol. 74, no. 3, pp. 409–427, 2001.

[37] E. E. Auer, K. W. Doak, and I. J. Schaffner, "Factors affecting laboratory cut-growth resistance of cold sbr tread stocks," *Rubber Chemistry and Technology*, vol. 31, no. 1, pp. 185–201, 1958.

[38] K. Cho, W. J. Jang, D. Lee, H. Chun, and Y.-W. Chang, "Fatigue crack growth of elastomers in the swollen state," *Polymer*, vol. 41, no. 1, pp. 179–183, 2000.